CARBON 74 (2014) 153–162

Available at www.sciencedirect.com

ScienceDirect

journal homepage: www.elsevier.com/locate/carbon

High-capacity graphene oxide/graphite/carbon nanotube composites for use in Li-ion battery anodes

Jingxian Zhang [a,b], Zhengwei Xie [a,b], Wen Li [a,b], Shaoqiang Dong [a,b], Meizhen Qu [a,*]

[a] Chengdu Institute of Organic Chemistry, Chinese Academy of Sciences, Chengdu 610041, PR China
[b] University of Chinese Academy of Sciences, Beijing 100039, PR China

ARTICLE INFO

Article history:
Received 6 November 2013
Accepted 7 March 2014
Available online 24 March 2014

ABSTRACT

A composite of graphene oxide sheets, carbon nanotubes (CNTs), and commercial graphite particles was prepared. The composite's use as a high-capacity and binder-free anode material for Li-ion batteries was examined. Results showed that this novel composite had a very high reversible Li-storage capacity of 1172.5 mA h g^{-1} at 0.5C (1C = 372 mA g^{-1}), which is thrice that of commercial graphite anode. The composite also exceeded the theoretical sum of capacities of the three ingredients. More importantly, its reversible capacity below 0.25 V can reach up to 600 mA h g^{-1}. In summary, the graphene oxide/graphite/CNT composite had higher reversible capacity, better cycling performance, and similar rate capability compared with the graphene oxide/graphite composite.

1. Introduction

Rechargeable Li-ion batteries (LIBs) are widely used in portable electronic devices and electric vehicles. Electrode materials are the key components responsible for the electrochemical properties of LIBs. Currently, the anode material of commercial LIBs is based on graphite because of the latter's excellent stability [1], safety [2], and affordability. However, graphite has a maximum theoretical Li-storage capacity of only 372 mA h g^{-1} [3], which hardly satisfies the changing requirements of portable electronic devices and recently developed fully electric vehicles. To improve the capacity, life cycle, and rate capability of LIBs, a considerable number of studies has focused on advanced carbonaceous materials, including mesophase carbon micro beads (MCMB) [4], hard carbon materials [5], carbon nanofibers [6], carbon nanotubes (CNTs) [7], and graphene [8]. However, reports on the direct use of graphene oxide as anode material in LIBs are limited.

In our previous work, we have shown that graphene oxide can be directly used in LIBs [9]. As a possible anode material, graphene oxide demonstrates an excellent performance, with a high capacity of 704.7 mA h g^{-1} at a current rate of 0.5C (1C = 372 mA g^{-1}). However, graphene oxide is unstable when subjected to electrochemical cycling after its compositing with commercial graphite. In the present study, we added CNTs to the above composite in an attempt to enhance its capacity, with the consideration that CNTs often used as conductive additives [10] possess a special one-dimensional (1D) structure, high electrical conductivity, and good transfer channels.

By compositing graphene oxide, graphite, and CNTs with the conductive additive (denoted as GGCC), a binder-free anode material with a high specific capacity was successfully

* *Corresponding author:* Fax: +86 2885215069.
E-mail address: mzhqu@cioc.ac.cn (M. Qu).
http://dx.doi.org/10.1016/j.carbon.2014.03.017
0008-6223/

synthesized. Compared with commercial anode materials that require polymeric binders and negatively affect the cost, specific capacity, and conductivity of LIBs [1], our GGCC composite can be directly used as an electrode without a need for any other binder. As such, our composite presents a solution to the abovementioned problems. Furthermore, graphite particles and CNTs were homogeneously distributed throughout graphene oxide sheets, which effectively prevented the restacking of the said sheets and promoted the easier movement of electrons within the electrode. Results of electrochemical tests indicated that the novel GGCC composite had very high reversible capacity, excellent rate capability, and cycling stability.

2. Experimental

2.1. Synthesis of materials

All chemical reagents used to prepare graphene oxide were analytical grade (purchased from Chengdu Kelong Chemicals Co., Ltd.) and used as received. Graphene oxide was synthesized from high-purity natural graphite flakes (about 200 meshes, 99.999% purity; Changsha Shenghua Research Institute) using the Hummers method [11]. In a typical synthesis, 5 g of natural graphite flakes was added to 115 ml of H_2SO_4 (98%) with vigorous stirring in an ice bath. Then, 15 g $KMnO_4$ was slowly added to the reaction vessel five times. Afterwards, 230 ml of deionized water and 30 ml of H_2O_2 were added to the suspension. The ice bath was removed and then subjected to centrifugal separation and repeated washing using dilute hydrochloric acid and deionized water. The colloidal dispersion of the as-synthesized graphene oxide in deionized water at a concentration of 1 mg ml^{-1} was prepared with the aid of ultrasonication (20 kHz ultrasound probe) for about 15 min until stabilization and browning of the dispersion.

The CNTs used in the GGCC composite were multi-walled CNTs purchased from Chengdu Organic Chemicals Co., Ltd. (CAS). The conductive additive used in the GGCC composite was Super-P carbon black (SP; 40 nm, 62 $m^2 g^{-1}$), purchased from TIMCAL Graphite & Carbon Co. The commercial graphite (characterized in Fig. 1a) used in the GGCC composite was purchased from BTR New Energy Materials Inc., Shenzhen (diameter, 8–15 μm; pellet density, 1.45–1.60 g cm^{-3}). For electrochemical tests, anode slurries were prepared by mixing adequate deionized water with the GGCC composite. The battery performances of the composites highly depended on the graphene oxide/graphite/CNT weight ratios. The highest capacities were obtained in from the composite with graphene oxide, graphite, CNT, and SP mass ratios of 15:60:20:5. The slurry was prepared by mixing adequate deionized water with the GGCC composite under vigorous stirring for 3 h. The resultant slurry was uniformly pasted onto a Cu foil with a blade. The prepared electrode sheets were dried at 120 °C in a vacuum oven for 12 h and subjected to a pressure of approximately 200 kg cm^{-2}. The electrodes of graphene oxide, graphite, and CNTs were prepared using the same processes with (a) graphene oxide and SP at a weight ratio of 85:15; (b) graphite, carboxymethyl cellulose (CMC; MW, 90,000; Aldrich), and SP at a weight ratio of 85:10:5; and (c) CNTs, CMC, and SP at a weight ratio of 85:10:5.

2.2. Characterization

The morphology and structure of the obtained samples were determined by scanning electron microscopy (SEM; INCA PentaFETx3) with energy-dispersive X-ray spectrometry (EDS) and transmission electron microscopy (TEM; JEM-100CX JEOL). X-ray photoelectron spectroscopy (XPS; PHI5600 Physical Electronics) was performed using Al/Kα radiation ($h\nu$ = 1486.6 eV) to determine elemental compositions and assignments of carbon peaks. X-ray diffraction (XRD) patterns were obtained from X'Pert MPD DX2700 using Cu/Kα radiation (λ = 1.5406 Å). Nitrogen adsorption–desorption isotherms at −196 °C were obtained using a Builder SSA4200 apparatus. Specific surface areas and porosimetries were calculated using the Brunauer–Emmett–Teller and Barrett–Joyner–Halenda methods based on the adsorption branches of the isotherms (Supplementary materials Fig. S1).

2.3. Electrochemical measurements

Electrochemical measurements were conducted using two-electrode CR2032 coin cells assembled in an argon-filled glove box. The electrolyte, obtained from Capchem Technology (Shenzhen) Co., Ltd., consisted of a solution of 1 M $LiPF_6$ in ethylene carbonate, dimethyl carbonate, diethyl carbonate (1:1:1, v/v). The separator used in the battery was Celgard 2400. A Li foil was used as the counter and reference electrode. Galvanostatic charge and discharge experiments were conducted at various rates on a BS-9300R battery test system within the potential range of 0.01–3.0 V versus Li^+/Li. Electrochemical impedance spectroscopy (EIS) and cyclic voltammetry (CV) tests were performed on a PARSTAT 2273 workstation.

3. Results and discussion

3.1. Characterization of materials

Fig. 1a and b present the micro-appearance of commercial graphite particles and multi-walled CNTs with an outer diameter of about 20–50 nm. Fig. 1c and d show the SEM and TEM images of the as-synthesized two-dimensional paper-like graphene oxide sheets. Fig. 1c shows that the oven-dried graphene oxide sheets easily form a soluble aggregate. After ultrasonication in deionized water (Fig. 1d), a nearly single layer of graphene oxide sheet is obtained from the aggregate. Corrugation and scrolling are part of the intrinsic nature of graphene oxide sheets. As such, nanovoids and nanocavities are to be expected in the GGCC composite. Fig. 1e shows that the rough surface of commercial graphite becomes smooth after compositing, indicating that it is uniformly wrapped by graphene oxide sheets. Moreover, at the junction of two graphite particles, the CNTs partly or fully wrapped by graphene oxide sheets make a bridge and form a conductive network. This structure helps enhance electron transfer between graphite particles and between graphene oxide sheets. More importantly, no obvious agglomeration is observed. Graphene oxide maintains its typical wrinkled paper-like structure after compositing with graphite and CNTs. The TEM image shown in Fig. 1f confirms this effect of the GGCC composite. Graphene oxide sheets cover the

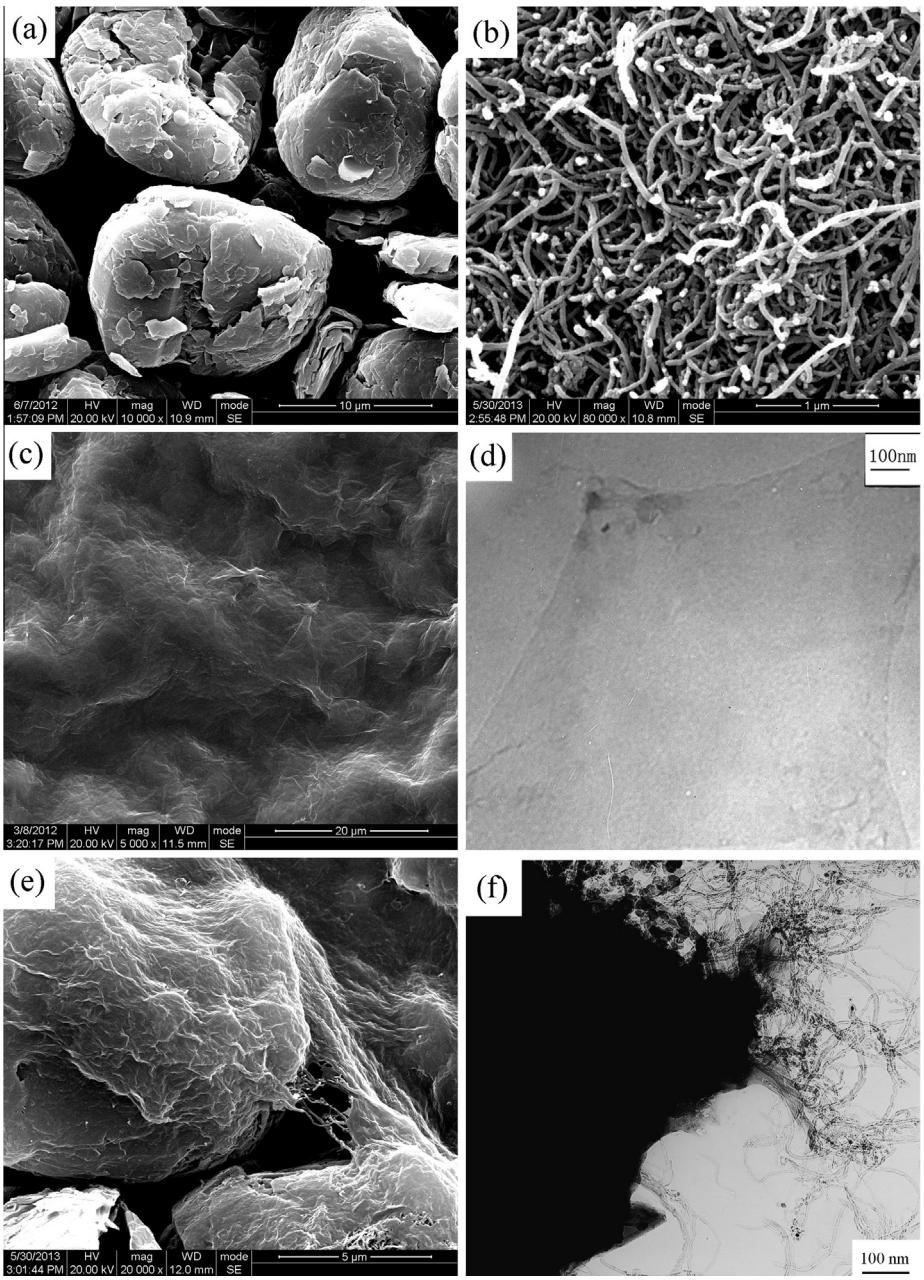

Fig. 1 – SEM images of (a) graphite, (b) CNT, (c) graphene oxide, and (e) GGCC composite. TEM images of (d) graphene oxide and (f) GGCC composite.

graphite particle and CNTs, and the latter are randomly aligned to form a conductive bridge.

Fig. 2a–c show the C1s XPS spectra of graphene oxide, CNT, and GGCC electrodes before discharge–charge tests. Fig. 2d and e display the C1s XPS spectrum of the GGCC electrode after being subjected to the initial charge (delithiation) and discharge (lithiation) test. Here in XPS analysis, Ar^+ sputtering is used to remove the influence of SEI film for the electrode which has undergone discharge–charge test. Graphene oxide shows four peaks at 284.6, 285.7, 286.8, and 287.8 eV (Fig. 2a), which correspond to sp^2 hybridized carbon, C—OH/C—N, C=O and O—C=O species, respectively [12]. Fig. 2b shows that the peaks at 284.6, 285.5, 286.9, 289.1, and 291.2 eV correspond to sp^2 hybridized carbon, C—OH/C—N, C=O, O—C=O and Ph–π^* species [13,14], respectively. As shown in Fig. 2c, all characteristic peaks of both graphene oxide and CNTs are found in the spectra of the GGCC composite. Five dominant peaks occur at 284.6, 285.9, 286.9, 288.5, and 290.3 eV, which correspond to sp^2 hybridized carbon, C—OH/C—N, C=O, O—C=O and Ph–π^* species, respectively. However, after the GGCC composite is subjected to a discharge–charge process at 0.1C, certain changes occur in the functional groups. A comparison of the peaks in Fig. 2c and d (both in delithiated state) suggests the following. First, a new peak of nearly semi-ionic C—F [15] group arises. Second, the peaks of C—OH/C—N, C=O and O—C=O show

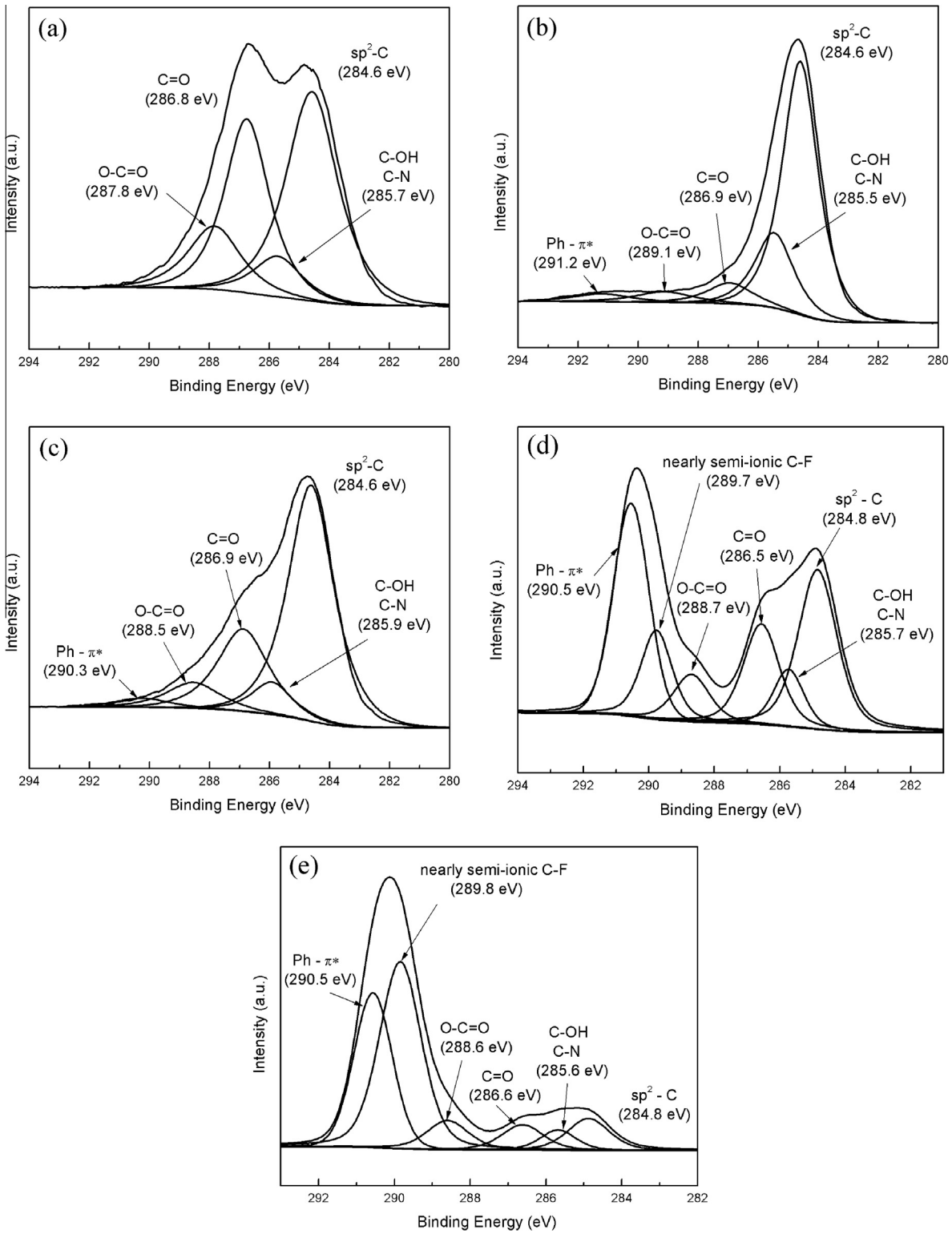

Fig. 2 – C1s XPS of (a) graphene oxide, (b) CNT, (c) GGCC electrode before electrochemical tests, (d) delithiated GGCC electrode, and (e) lithiated GGCC electrode at 0.1C.

unconspicuous change but shifts to a slightly lower binding energy. Third, the peak of Ph–π^* noticeably increases after the electrochemical test. While in comparison of Fig. 2d and e, the peak intensity of sp^2 hybridized carbon, semi-ionic C—F, C═O, C—OH/C—N and Ph–π^* groups have changed obviously after lithiation process, which may mean above groups have the ability of bonding Li-ion in the full lithiated state of GGCC electrode.

3.2. *Electrochemical characterization of materials*

The discharge–charge behavior of graphene oxide, CNT, graphite, and the GGCC electrodes in a constant current mode at 0.5C are shown in Fig. 3a–d. Based on the first discharge curve of graphene oxide electrode in Fig. 3a, the capacity below 0.5 V is primarily attributed to Li intercalation in the graphene oxide layers [16]. By contrast, the capacity above 0.5 V can be ascribed to faradic capacitance or side reactions [17], such as the formation of a SEI film. The discharge–charge behavior of CNT electrode in Fig. 3b is similar to that of graphene oxide electrode. Two slopes emerge in the first discharge curve of CNT electrode from 1.8 to 1.0 V and from 1.0 to 0.7 V, which can be ascribed to the lithiation side reaction in CNTs and SEI layer formation. Fig. 3c shows the typical discharge–charge profile of graphite electrode, which has been analyzed in previous reports [18]. As shown in Fig. 3d, the discharge–charge behavior of GGCC electrode after it has been composited with graphene oxide, graphite, and CNTs exhibits all the features of the three electrodes above, although some plateaus overlap with each other. GGCC electrode delivers a very high specific capacity of 1942.6 mA h g^{-1} in the initial discharging and a reversible capacity of 1153.7 mA h g^{-1} in the first charging. To the best of our knowledge, such extremely high reversible capacity at the current rate of 0.5C exceeds almost all previously reported ones for graphite-composited carbonaceous materials, such as MCMB [19], nitrogen-doped chemically reduced mesocarbon microbead oxide [20], and graphite/Si-based composite [21–23] (Table S1, Supplementary materials).

Besides the normal LiC_6 storage, the high capacity yielded from GGCC composite may comprise: (a) LiC_2 storage [24]. Graphene oxide in GGCC composite still has the graphite layer structure and high proportion of aromatic ring (sp^2 hybridized carbon) is contained, which is confirmed by XRD, EDS and XPS results (Figs. S2 and S3 of Supplementary material). So just like graphene, the LiC_2 storage mode is very possible. (b) Lithium storage in nano-cavity. In the GGCC composite, CNTs and SP conductive additive are uniformly dispersed among the graphene oxide sheets, and the interface between graphite and graphene oxide. The present of CNTs and SP particles can effectively enhance the electric conductivity of the composite on one hand, and create some nano pore and channel structures on the other, which also have the storage capacity of lithium [25]. (c) Lithium storage in surface functional groups, and above XPS results has proved this. The role of

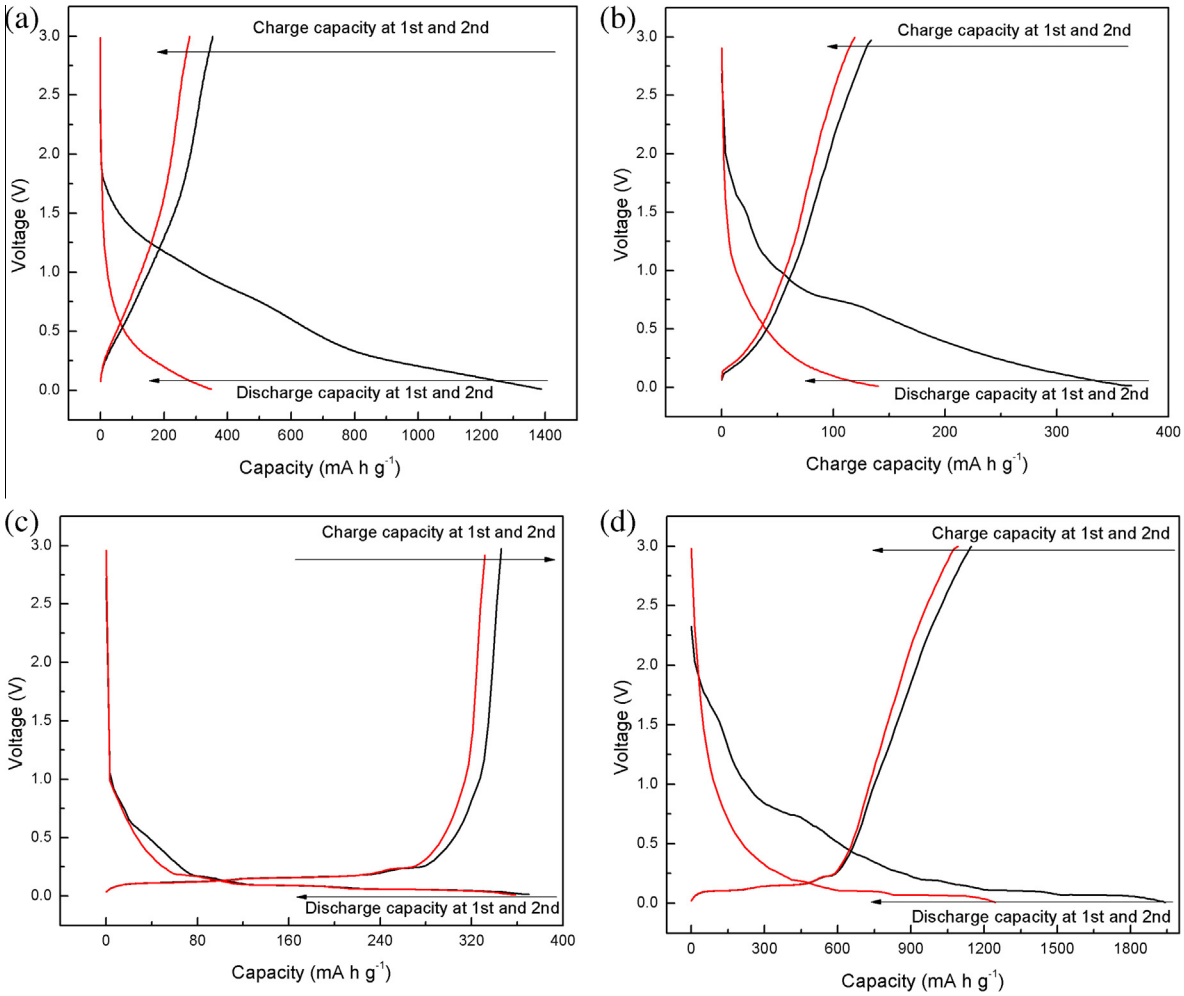

Fig. 3 – First two discharge–charge profiles of (a) graphene oxide, (b) CNT, (c) graphite, and (d) GGCC electrodes. (A color version of this figure can be viewed online.)

functional groups in providing high capacity in GGCC composite is further confirmed by comparing the specific capacity of GGCC, reduced-GGCC (RGGCC, exposure to 10% H_2 and 90% Ar by volume at 400 °C for 3 h, employing 10 wt % carboxymethyl cellulose (CMC) binder) and GGCC–CMC electrode (GGCC with 10 wt% CMC binder). The discharge–charge test result (Fig. S4 of Supplementary material) shows that, at different current rate, the specific capacity is in a sequence of GGCC > GGCC–CMC > RGGCC, indicating a dominant contribution to the capacity from the surface functional groups [12]. Furthermore, the enhanced conductivity may be helpful for lessening polarization so as to increase specific capacity, and the faradic capacitance can also contribute to lithium storage [26].

Compared with our previous work, the present results indicate that the charge capacity of the GGCC composite has an improvement of >55% over that of the graphene oxide/graphite composite, which exhibits an initial discharge and charge capacity of 1039.4 and 704.7 mA h g^{-1} [9], respectively. Thus, the addition of CNTs significantly boosts the Li-storage capacity of the GGCC composite. Furthermore, the GGCC electrode's capacity below 0.25 V can reach as high as 600 mA h g^{-1}, which is much higher than the theoretical sum of capacities below 0.25 V of the three ingredients (295.8 mA h g^{-1}). This finding suggests the occurrence of a synergistic interaction among graphene oxide, graphite, and CNTs, which requires further investigation.

However, GGCC electrode notably exhibits poor initial coulombic efficiency (the percentage ratio of charge-to-discharge capacity) of only 58% under a current rate of 0.5C. This behavior suggests the low efficiency of the ingredient electrodes, such as graphene oxide (37%) and CNTs (42%). The Li-ion irreversible consumption in the formation of the SEI layer of both electrodes is very high as a result of their large surface area [27,28]. Furthermore, certain side reactions also need to be considered, such as the electrochemical reduction of residual oxygen-containing functional groups in the materials, as proven by the XPS spectra (Fig. 2d). To improve the coulombic efficiency of the as-synthesized GGCC anode material, we have explored a variety of approaches, such as electric plating and mild pre-reduction. The results of these explorations are to be collected and reported in the future.

Fig. 4 shows the CV data of graphene oxide, CNT, graphite, and GGCC electrodes conducted at a scan rate of 0.1 mV s^{-1} from 0.01 to 3.0 V vs. Li^+/Li. In Fig. 4a, a large reductive peak from 2.0 to 0.5 V is observed for graphene oxide electrode in

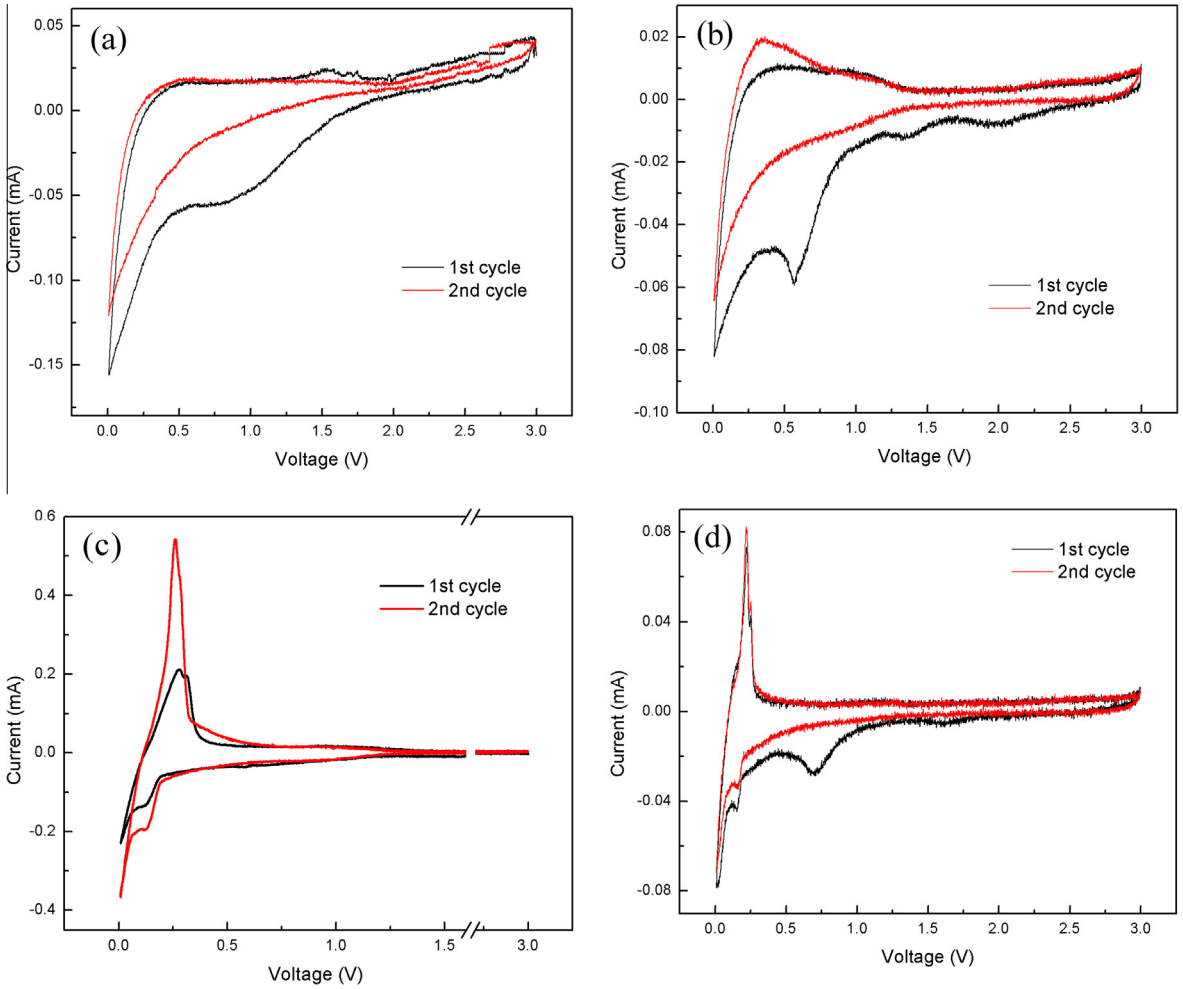

Fig. 4 – First two cyclic voltammograms of (a) graphene oxide, (b) CNT, (c) graphite, and (d) GGCC electrodes. (A color version of this figure can be viewed online.)

the first cycle, and this peak corresponds to the formation of SEI film and the reduction of trace water or oxygen groups [29] that disappear in the second cycle. Moreover, the peak intensity and area from 0.5 to 0.01 V in the second cycle is weaker than that in the first cycle, indicating some fading of active Li storage sites, for instance, the aggregation of graphene oxide sheets after the electrochemical test. Fig. 4b presents the CV profiles of CNT electrode. In the first cycle, two small negative current peaks occur at about 2.0 and 1.3 V. These peaks possibly result from the reduction of trace water and surface groups on the CNT surface [30], both of which are observable only in the first cycle. The distinct reduction current peak at about 0.6 V can be attributed to SEI formation [31]. As expected, this peak is reduced in the subsequent cycle. The CV profile of graphite electrode (Fig. 4c) is interpreted in detail in a previous article [32]. The CV measurement of GGCC electrode in Fig. 4d shows that Li can reversibly intercalate and deintercalate with the composite. In the first cycle, two peaks emerge at about 1.7 and 0.7 V. The former can be ascribed to the electrochemical reduction of oxygen groups in the composite, and the latter can be attributed to the formation of SEI film on composite surface [33]. This formation is associated with electrolyte decomposition and the formation of Li organic compounds. Such peaks are not detected in the subsequent cycle. The peak close to 0 V corresponds to the intercalation of Li with graphene oxide, graphite, and CNTs, a typical feature of Li–carbon interaction [34]. The CV measurements confirm the reversible electrochemical reaction between Li ions and the GGCC composite in Li-ion cells.

Fig. 5a presents the cycle performances of graphene oxide, graphite, CNT, and GGCC electrodes at 0.5C. The capacity of graphene oxide electrode sharply decreases in the first few cycles and slightly declines in the subsequent cycles. Finally, the capacity reaches 148.7 mA h g^{-1} after 60 cycles, and its correlated capacity retention rate is 39.8%. By contrast, both graphite and CNT electrodes show very stable cycle performance with only a slight increase in capacity. However, their capacities are only 344.5 and 149.3 mA h g^{-1} after 60 cycles. After compositing all three ingredients, GGCC electrode exhibits very high reversible capacity and stable cycle performance. This electrode shows an initial capacity of 1172.5 mA h g^{-1} and a final capacity of 1050.3 mA h g^{-1} in the 60th cycle, yielding an extremely high capacity retention of 89.6% (86.9% for 325 cycle times in Supplementary material Fig. S5). Moreover, as shown in Fig. 5b, GGCC electrode is a great improvement in the graphene oxide/graphite composite

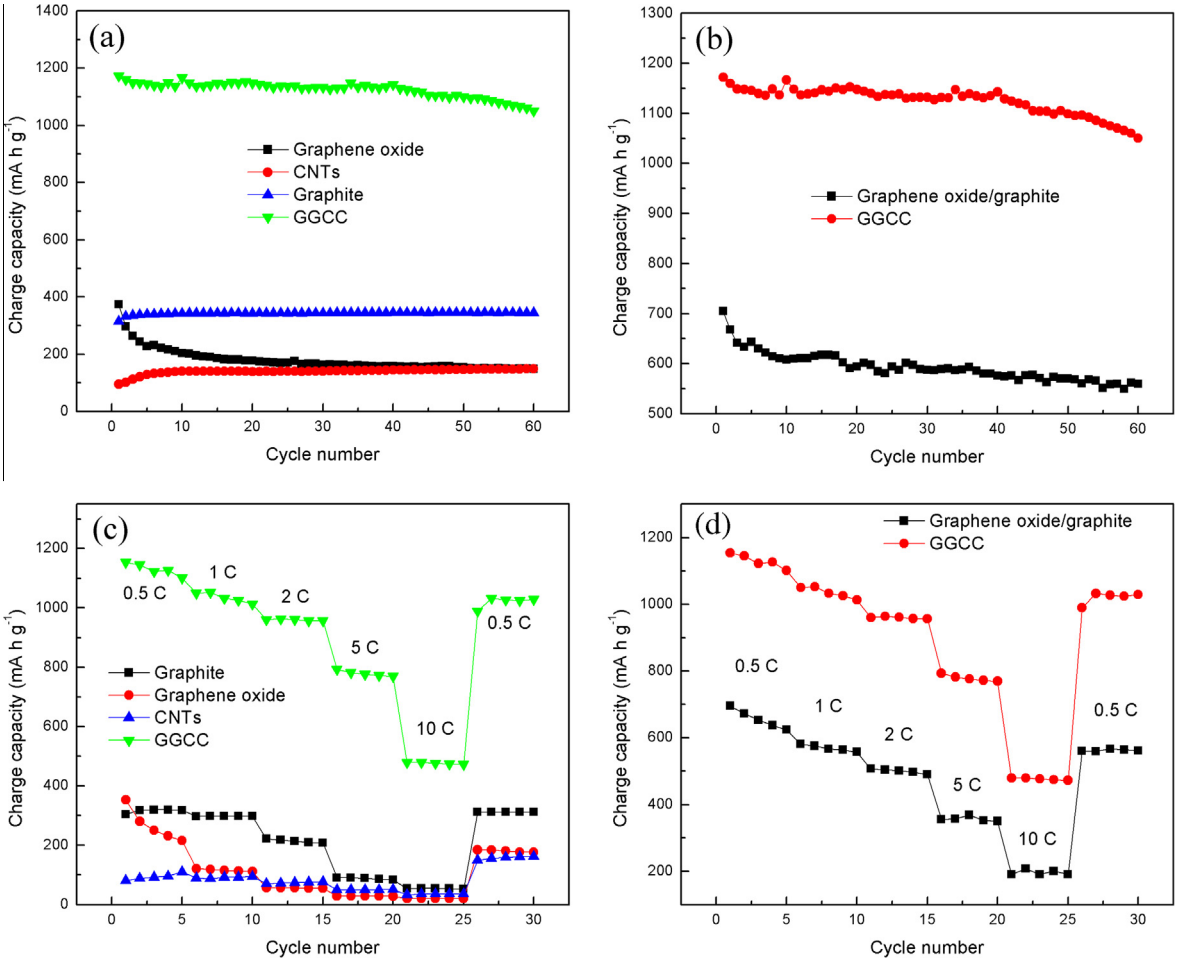

Fig. 5 – Cyclic performance of (a) graphene oxide, graphite, CNT, and GGCC electrodes; and (b) graphene oxide/graphite composite and GGCC electrodes. Rate capabilities of (c) graphene oxide, graphite, CNT, and GGCC electrodes; and (d) graphene oxide/graphite composite and GGCC electrodes. (A color version of this figure can be viewed online.)

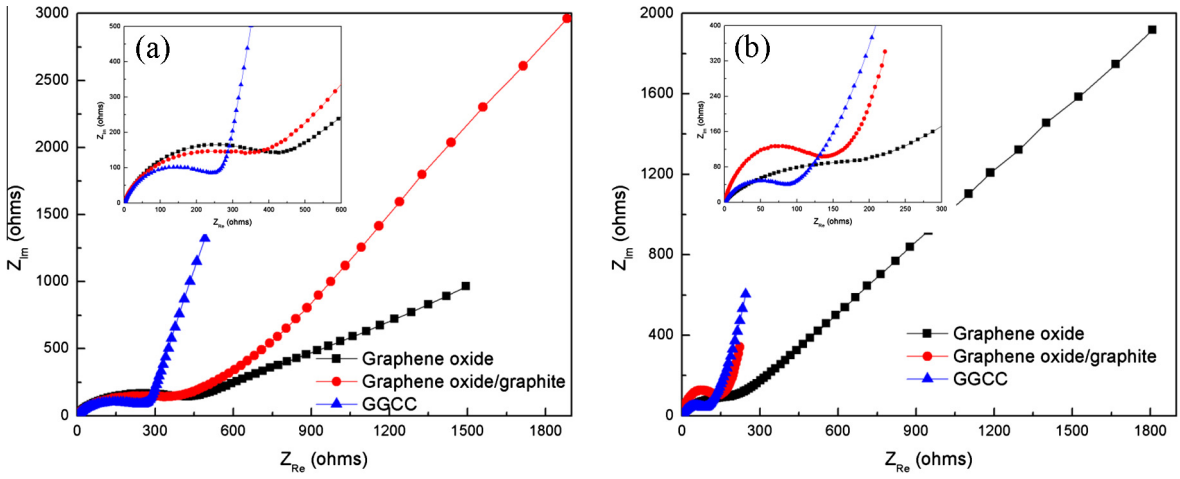

Fig. 6 – Nyquist plots of graphene oxide, graphene oxide/graphite composite and GGCC electrodes obtained by applying a sine wave amplitude of 10.0 mV over the frequency range of 10 kHz to 0.1 Hz: (a) before and (b) after two discharge–charge cycles at 0.1C. (A color version of this figure can be viewed online.)

electrode, which has a capacity of 559.3 mA h g^{-1} in the 60th cycle and a capacity retention of 79.4% based on our previous study [9]. Such an improvement is a result of the addition of CNTs, which have an outstanding conductive network that enhances both reversible capacity and cycle stability.

The rate capabilities of graphene oxide, graphite, CNT, and GGCC electrodes at various charge rates were also compared to test the superiority of GGCC composite. As Fig. 5c shows, graphene oxide electrode exhibits the lowest rate capability, markedly dropping from 353.1 mA h g^{-1} at 0.5C to 19.7 mA h g^{-1} at 10.0C. Similarly, the capacity of graphite electrode also drops from 303.8 mA h g^{-1} at 0.5C to 54.7 mA h g^{-1} at 10.0C. Although the capacity of CNT electrode slightly decreases with increased current rate, its capacity is very low (only 162.5 mA h g^{-1} at 0.5C and 35.1 mA h g^{-1} at 10.0C). By contrast, GGCC electrode is stable at different current rates and delivers capacities of 1153.7, 1049.9, 960.6, 793.1, and 478.8 mA h g^{-1} at 0.5C, 1.0C, 2.0C, 5.0C, and 10.0C, respectively. Clearly, GGCC electrode displays the highest charge capacity and preferable capacity retention with increased current rate, signifying the synergistic effect of compositing the original components. After cycling at various rates with the current density back at 0.5C, the capacities of all the electrodes, except that of graphene oxide, revert to their original values, suggesting good reversibility and structure stability. The rate capability of the graphene oxide/graphite composite was also compared with that of GGCC electrode, and the results are presented in Fig. 5d. The capacity of GGCC electrode is much higher than that of graphene oxide/graphite composite electrode at any current rate. This result further confirms the importance of adding CNTs, which effectively form a conductive network and improve rate capability.

The powerful technique of EIS was also used to evaluate the electrochemical behavior of graphene oxide, graphene oxide/graphite composite and GGCC electrodes. Fig. 6a and b show the EIS of the three electrodes before and after discharge–charge processes. The insets are high-frequency region Nyquist plots. The EIS of these electrodes consist of a quasi-semicircle from high to middle frequency, which can be attributed to the charge transfer processes on the electrode–electrolyte interface, and of a straight sloping line in the low-frequency range, which indicates the impedance caused by the Li diffusion and accumulation processes in the working electrode. The former is associated with the porous structure of the electrodes, and the latter is the characteristic feature of pure capacitive behavior [35]. The numerical value of the diameter of the semicircle on the Z_{Re} axis gives an approximate indication of the charge-transfer resistance (R_{ct}). As shown in Fig. 6a, the R_{ct} of GGCC electrode (238.8 Ω) is much lower than that of graphene oxide (425.8 Ω) and graphene oxide/graphite composite (334.9 Ω) electrode before discharge–charge processes. This results indicate that the addition of CNTs could help form a conductive network and facilitate the movement of electrons. However, after discharge–charge processes (Fig. 6b), the R_{ct} of GGCC electrode markedly decreased to 82.6 Ω, whereas that that of graphene oxide and graphene oxide/graphite composite electrode decrease to 185.7 and 134.3 Ω. This finding can be explained by the electrochemical reduction of oxygen groups on the surface of graphene oxide sheets, which occurs during the discharge–charge process that increases the electric conductivity of graphene oxide and GGCC electrodes [36]. The good electrolyte wetting after the discharge–charge process, which results in a large contact area between the active material and electrolyte, also needs to be considered [37].

4. Conclusions

A novel composite of graphene oxide, graphite, and CNTs was successfully synthesized. This GGCC composite can be directly used as a binder-free anode material. Based on electrochemical measurements, the composite exhibits superior performance and stable properties, with a capacity of 1050.3 mA h g^{-1} after 60 cycles at a rate of 0.5C and a rate capacity of 478.8 mA h g^{-1} at a current rate of 10.0C. Its reversible capacity below 0.25 V (vs. Li^+/Li) is almost 600 mA h g^{-1}, whereas the theoretical sum of the reversible capacity of graphene oxide, graphite, and CNTs is only

295.8 mA h g^{-1}. The GGCC composite shows a larger reversible capacity with higher capacity retention and rate capability than previously reported graphene oxide/graphite composites. These performance enhancements mostly result from the addition of CNTs, which help form a conductive network and facilitate the movement of electrons. Moreover, the synergistic effect of compositing graphene oxide, graphite, and CNTs is noted. Based on galvanostatic discharge–charge, CV, and EIS studies, we conclude that the use of the as-synthesized material as an anode material for LIBs is not only viable but also desirable.

Author contributions

Meizhen Qu planed and supervised the project. Jingxian Zhang conceived and performed the experiments, analyzed the results and wrote the paper. Zhengwei Xie helped with synthesis and characterization of the materials. Wen Li analyzed and collected the data. Shaoqiang Dong, Zhengwei Xie and Wen Li all discussed the results and commented on the manuscript. All authors discussed the results and commented on the manuscript.

Acknowledgement

This work was conducted with financial support from Ministry of Science and Technology (MOST) of China (2011CB932604).

Appendix A. Supplementary data

Supplementary data associated with this article can be found, in the online version, at http://dx.doi.org/10.1016/j.carbon.2014.03.017.

REFERENCES

[1] Lahiri I, Oh SW, Hwang JY, Cho S, Sun YK, Banerjee R, et al. High capacity and excellent stability of lithium ion battery anode using interface-controlled binder-free multiwall carbon nanotubes grown on copper. ACS Nano 2010;4(6):3440–6.
[2] Abouimrane A, Compton OC, Amine K, Nguyen ST. Non-annealed graphene paper as a binder-free anode for lithium-ion batteries. J Phys Chem C 2010;114(29):12800–4.
[3] Ji L, Lin Z, Alcoutlabi M, Zhang X. Recent developments in nanostructured anode materials for rechargeable lithium-ion batteries. Energy Environ Sci 2011;4(8):2682–99.
[4] Zhang HL, Sun CH, Li F, Liu C, Tan J, Cheng HM. New insight into the interaction between propylene carbonate-based electrolytes and graphite anode material for lithium ion batteries. J Phys Chem C 2007;111(12):4740–8.
[5] Buiel E, Dahn JR. Li-insertion in hard carbon anode materials for Li-ion batteries. Electrochim Acta 1999;45(1–2):121–30.
[6] Liwen J, Xiangwu Z. Fabrication of porous carbon nanofibers and their application as anode materials for rechargeable lithium-ion batteries. Nanotechnology 2009;20(15):155705.
[7] Landi Brian J, G MJ, Cress Cory D, DiLeo Roberta A, Raffaelle Ryne P. Carbon nanotubes for lithium ion batteries. Energy Environ Sci 2009;2(6):638–54.
[8] Bhardwaj Tarun, A A, Pavan Barbara, Barone Veronica, Fahlman Bradley D. Enhanced electrochemical lithium storage by graphene nanoribbons. J Am Chem Soc 2010;132(3):12556–8.
[9] Zhang J, Cao H, Tang X, Fan W, Peng G, Qu M. Graphite/graphene oxide composite as high capacity and binder-free anode material for lithium ion batteries. J Power Sources 2013;241:619–26.
[10] Li X, Kang F, Shen W. Multiwalled carbon nanotubes as a conducting additive in a $LiNi_{0.7}Co_{0.3}O_2$ cathode for rechargeable lithium batteries. Carbon 2006;44(7):1298–352.
[11] Hummers WS, Offeman RE. Preparation of graphitic oxide. J Am Chem Soc 1958;80(6):1339.
[12] Lee SW, Yabuuchi N, Gallant BM, Chen S, Kim BS, Hammond PT, et al. High-power lithium batteries from functionalized carbon-nanotube electrodes. Nat Nanotechnol 2010;5:531–7.
[13] Shao Y, Wang J, Engelhard M, Wang C, Lin Y. Facile and controllable electrochemical reduction of graphene oxide and its applications. J Mater Chem 2010;20(4):743.
[14] Kuo SL, Liu WR, Kuo CP, Wu NL, Wu HC. Lithium storage in reduced graphene oxides. J Power Sources 2013;244:552–6.
[15] Robinson JT, Burgess JS, Junkermeier CE, Badescu SC, Reinecke TL, Perkins FK, et al. Properties of fluorinated graphene films. Nano Lett 2010;10(8):3001–5.
[16] Wang G, Shen X, Yao J, Park J. Graphene nanosheets for enhanced lithium storage in lithium ion batteries. Carbon 2009;47(8):2049–53.
[17] Wu ZS, Ren W, Xu L, Li F, Cheng HM. Doped graphene sheets as anode materials with superhigh rate and large capacity for lithium ion batteries. ACS Nano 2011;5(7):5463–71.
[18] Yoshio M, Wang H, Fukuda K, Umeno T, Abe T, Ogumi Z. Improvement of natural graphite as a lithium-ion battery anode material, from raw flake to carbon-coated sphere. J Mater Chem 2004;14(11):1754–8.
[19] Courtel FM, Niketic S, Duguay D, Lebdeh AY, Davidson IJ. Water-soluble binders for MCMB carbon anodes for lithium-ion batteries. J Power Sources 2011;196(4):2128–34.
[20] Han P, Yue Y, Zhang L, Xu H, Liu Z, Zhang K, et al. Nitrogen-doping of chemically reduced mesocarbon microbead oxide for the improved performance of lithium ion batteries. Carbon 2012;50(3):1355–62.
[21] Lee HY, Lee SM. Carbon-coated nano-Si dispersed oxides/graphite composites as anode material for lithium ion batteries. Electrochem Commun 2004;6(5):465–9.
[22] Hu YS, Cakan DR, Titirici MM, Müller JO, Schlögl R, Antonietti M, et al. Superior storage performance of a Si@SiOx/C nanocomposite as anode material for lithium-ion batteries. Angew Chem Int Ed 2008;47(9):1645–9.
[23] Ji J, Ji H, Zhang LL, Zhao X, Bai X, Fan X, et al. Graphene-encapsulated Si on ultrathin-graphite foam as anode for high capacity lithium-ion batteries. Adv Mater 2013;25(33):4673–7.
[24] Sato K, Noguchi M, Demachi A, Oki N, Endo M. A mechanism of lithium storage in disordered carbons. Science 1994;264(5158):556–8.
[25] Peled E, Menachem C, Bar-Tow D, Melman A. Improved graphite anode for lithium-ion batteries chemically bonded solid electrolyte interface and nanochannel formation. J Electrochem Soc 1996;143(1):L4–7.
[26] Yoo EJ, Kim J, Hosono E, Zhou H, Kudo T, Honma I. Large reversible Li storage of graphene nanosheet families for use in rechargeable lithium ion batteries. Nano Lett 2008;8(8):2277–82.
[27] Wang G, Wang B, Wang X, Park J, Dou S, Ahn H, et al. Sn/graphene nanocomposite with 3D architecture for enhanced reversible lithium storage in lithium ion batteries. J Mater Chem 2009;19(44):8378–84.
[28] Zhao X, Hayner CM, Kung HH. Self-assembled lithium manganese oxide nanoparticles on carbon nanotube or

graphene as high-performance cathode material for lithium-ion batteries. J Mater Chem 2011;21(43):17297–303.
[29] Chou SL, Zhao Y, Wang JZ, Chen ZX, Liu HK, Dou SX. Silicon/single-walled carbon nanotube composite paper as a flexible anode material for lithium ion batteries. J Phys Chem C 2010;114(37):15862–7.
[30] Smart M, Ratnakumar B, Surampudi S. Electrolytes for low-temperature lithium batteries based on ternary mixtures of aliphatic carbonates. J Electrochem Soc 1999;146(2):486–92.
[31] Chew SY, Ng SH, Wang J, Novák P, Krumeich F, Chou SL, et al. Flexible free-standing carbon nanotube films for model lithium-ion batteries. Carbon 2009;47(13):2976–83.
[32] Wu YP, Rahm E, Holze R. Carbon anode materials for lithium ion batteries. J Power Sources 2003;114(2):228–36.
[33] Li X, Geng D, Zhang Y, Meng X, Li R, Sun X. Superior cycle stability of nitrogen-doped graphene nanosheets as anodes for lithium ion batteries. Electrochem Commun 2011;13(8):822–5.
[34] Kalbac M, Hsieh Y-P, Farhat H, Kavan L, Hofmann M, Kong J, et al. Defects in individual semiconducting single wall carbon nanotubes: Raman spectroscopic and in situ Raman spectroelectrochemical study. Nano Lett 2010;10(11):4619–26.
[35] Wang G, Zhang L, Zhang J. A review of electrode materials for electrochemical supercapacitors. Chem Soc Rev 2012;41(2):797–828.
[36] Giraudet J, Dubois M, Inacio J, Hamwi A. Electrochemical insertion of lithium ions into disordered carbons derived from reduced graphite fluoride. Carbon 2003;41(3):453–63.
[37] Wang X, Cao X, Bourgeois L, Guan H, Chen S, Zhong Y, et al. N-doped graphene-SnO2 sandwich paper for high-performance lithium-ion batteries. Adv Funct Mater 2012;22(13):2682–90.